

Forward, Reverse and FXMOTR Modeling of the LMO: A Look at the

Bulk Composition of the LMO

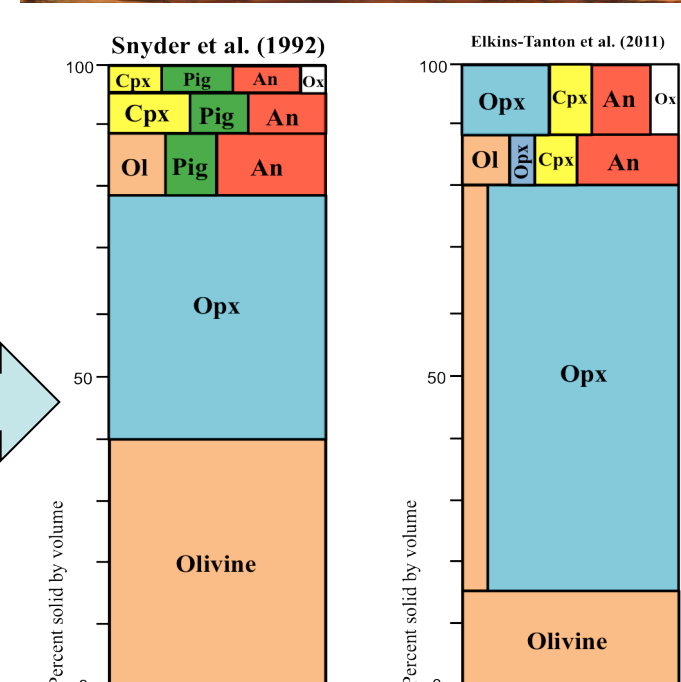
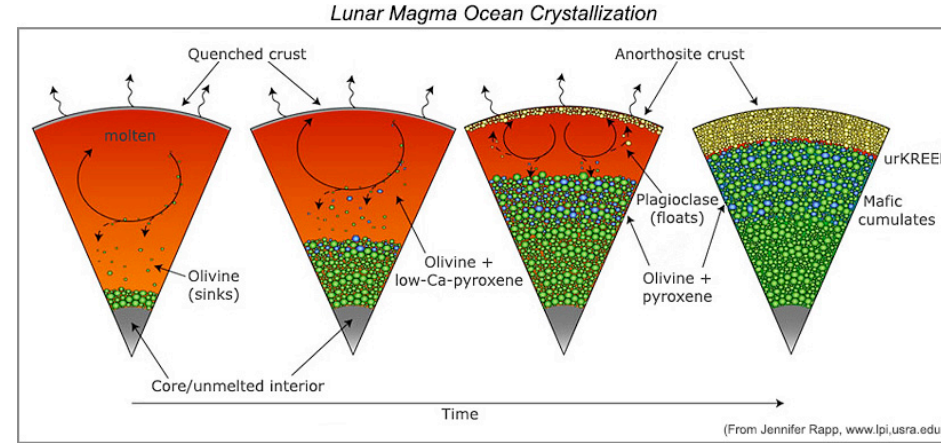
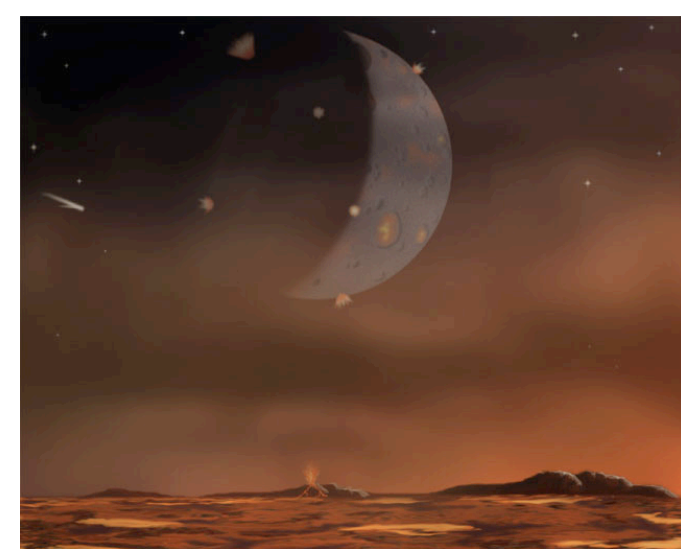
Jesse Davenport,^{1,2} Clive R. Neal,^{2,3} Gregory A. Snyder,⁴ Diogo Bolster,³ and John Longhi⁵

¹Centre de Recherches Pétrographiques et Géochimiques, Vadœuvre-les-Nancy, France 54500, ²NASA Lunar Science Institute, Center for Lunar Science and Exploration, LPI, Houston, TX 77058, ³CEES, University of Notre Dame, Notre Dame, IN 46556, U.S.A., ⁴3673 Maybank Highway, P.O. Box 125, Johns Island, SC 29457, U.S.A. ⁵Lamont-Doherty Earth Observatory, Palisades, NY 10964, U.S.A. (jessed@crpg.cnrs-nancy.fr; neal.1@nd.edu)



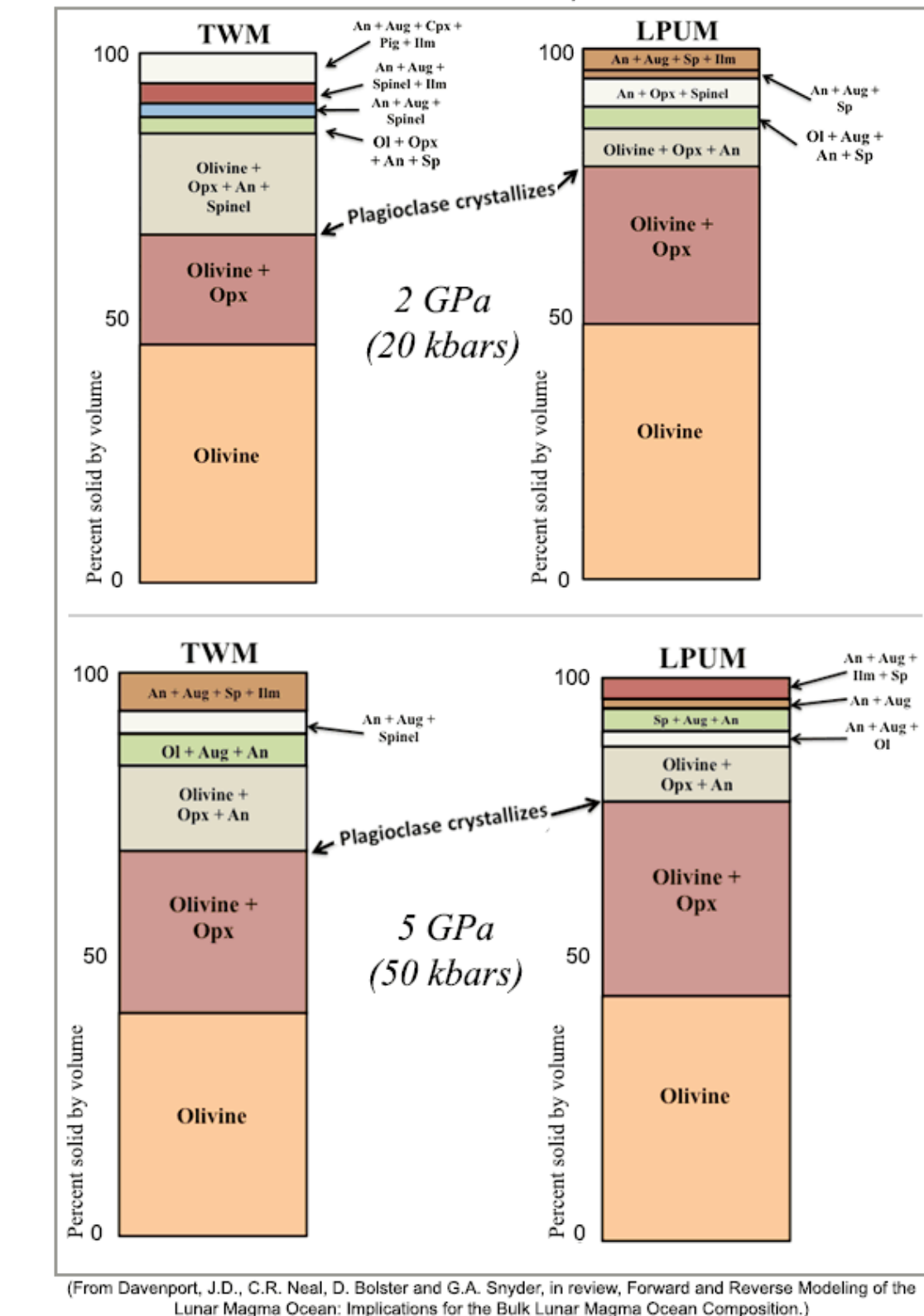
Introduction and Aim of Study

- The LMO is a key concept to understanding the origin and evolution of the Moon, Earth, and other terrestrial planets.
- LMO theory was first established with the return of anorthositic samples from the Apollo missions [1,2,3,4,5].



- Goal 1:** Recreate LMO model of [6] and vary parameters.
- Goal 2:** Construct a reverse LMO model [8].
- Goal 3:** Model LMO crystallization using FXMOTR and investigate presence of garnet in the Lunar Mantle [18].
- Numerical models = valuable tools for understanding LMO evolution.
- But... models must be combined with ground truth → sample and remote sensing.
- Important parameters must be considered to accurately describe the evolution of the LMO (e.g., Initial composition, depth of LMO).

Figure 7. Crystallization Order of the Lunar Magma Ocean Modeled for Two Compositions



FXMOTR Modeling

- Using FXMOTR [11], we varied LMO depth (and hence pressure; 2 GPa=400 km & 5 GPa=1000 km) and initial composition between Al-rich and poor compositions (Fig. 7).
- Al-rich compositions (i.e. TWM) produce plagioclase (~65 PCS) on the liquidus before LPUM (~78-80 PCS).
- [16], using MELTS, has proposed that the Moon is more enriched in FeO and Al₂O₃ than previously thought, consistent with our results.
 - They argue that bulk Moon FeO can be constrained to between 1.3 and 1.8 x Bulk Silicate Earth (BSE) and Al₂O₃ between 1 and 1.5 x BSE.
- FXMOTR consistently generates small quantities (~1-5 wt.%; below 500 km) of garnet in the lunar mantle with Al-rich bulk compositions ([18]).

Reverse Modeling

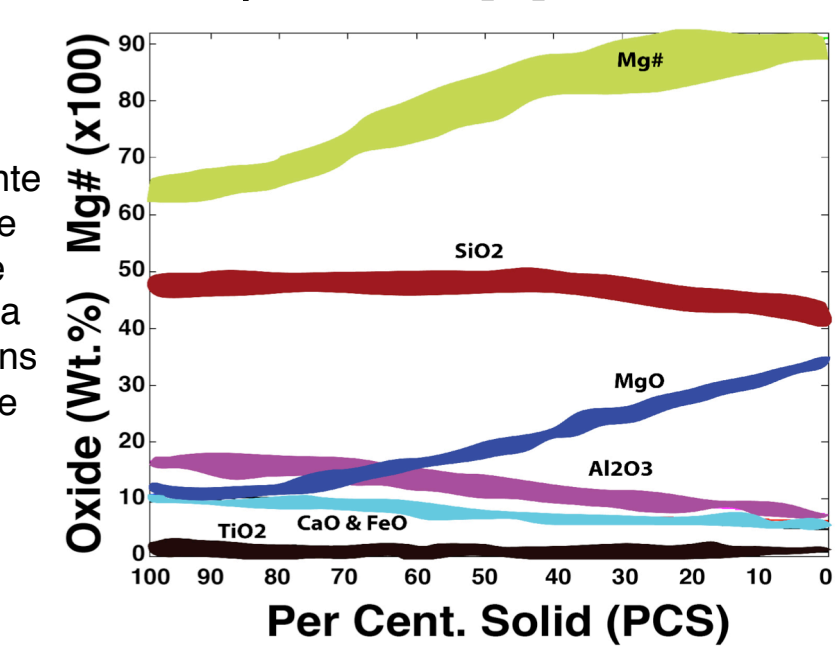
- Geochemical compositions of urKREEP and FAN are processed in a backwards fashion through various LMO models (Figs. 8-12; [8,9]).
- This allows an estimate of the bulk LMO to be calculated from ground truth, rather than starting with an assumed bulk composition [9].

urKREEP (Warren and Wasson, 1979)	
SiO ₂	47.96
TiO ₂	1.65
Al ₂ O ₃	16.63
FeO	10.58
MnO	0.14
MgO	10.62
CaO	9.52
Na ₂ O	0.86
K ₂ O	0.83
P ₂ O ₅	0.78
Cr ₂ O ₃	1.3



Figure 8 (left). A schematic of reverse LMO modeling.

Figure 11 (right). Reverse Monte Carlo modeling of LMO. A range of urKREEP compositions were generated in order to generate a range of initial LMO compositions (at 0 PCS). This is a very simple way to compare modeled initial LMO compositions with those generated from ground truth.



Forward Modeling

- [6] created a crystallization model (Fig. 2) of the LMO, but did not explain major or trace element modeling in detail.
- [6] shows a progressive depletion of MgO after 78 PCS (Percent Solid; Plag. on liquidus); subsequent, rapid depletion of Mg# (Fig. 3-6; TWM [12] & LPUM [13] for comparison).
- Trace element modeling is recreated here (Fig. 4).
- [6] predicts 0 wt% MgO for urKREEP, but calculated compositions predict ~10 wt% MgO (e.g., [10]).
- [9] predicts 7-10 wt% MgO for urKREEP with an appropriate Mg# to match (~.40).

Figure 2. Schematic of forward LMO modeling. A bulk LMO is crystallized through a specific sequence and the resulting final liquid compositions are compared to urKREEP compositions.

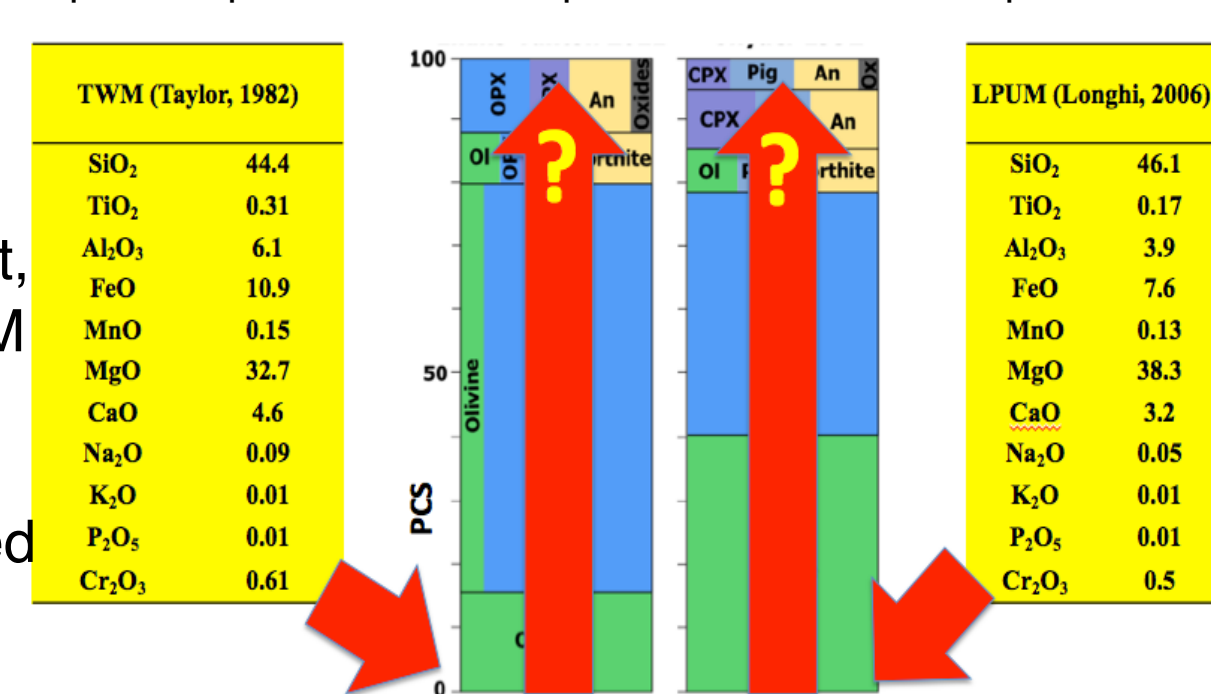


Figure 3. Major element evolution of the Lunar Magma Ocean. A) TWM evolution, B) [6] evolution, C) LPUM evolution and D) the recreation of [6].

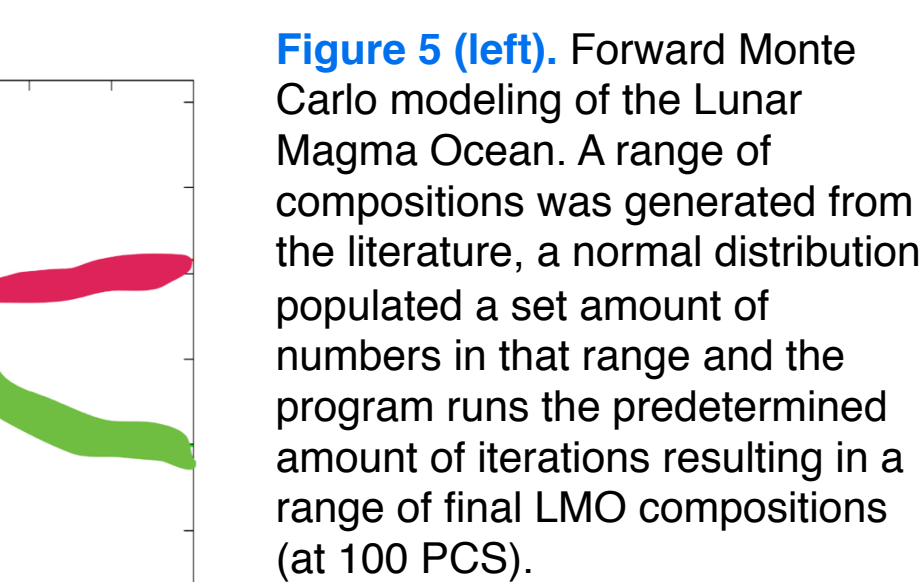
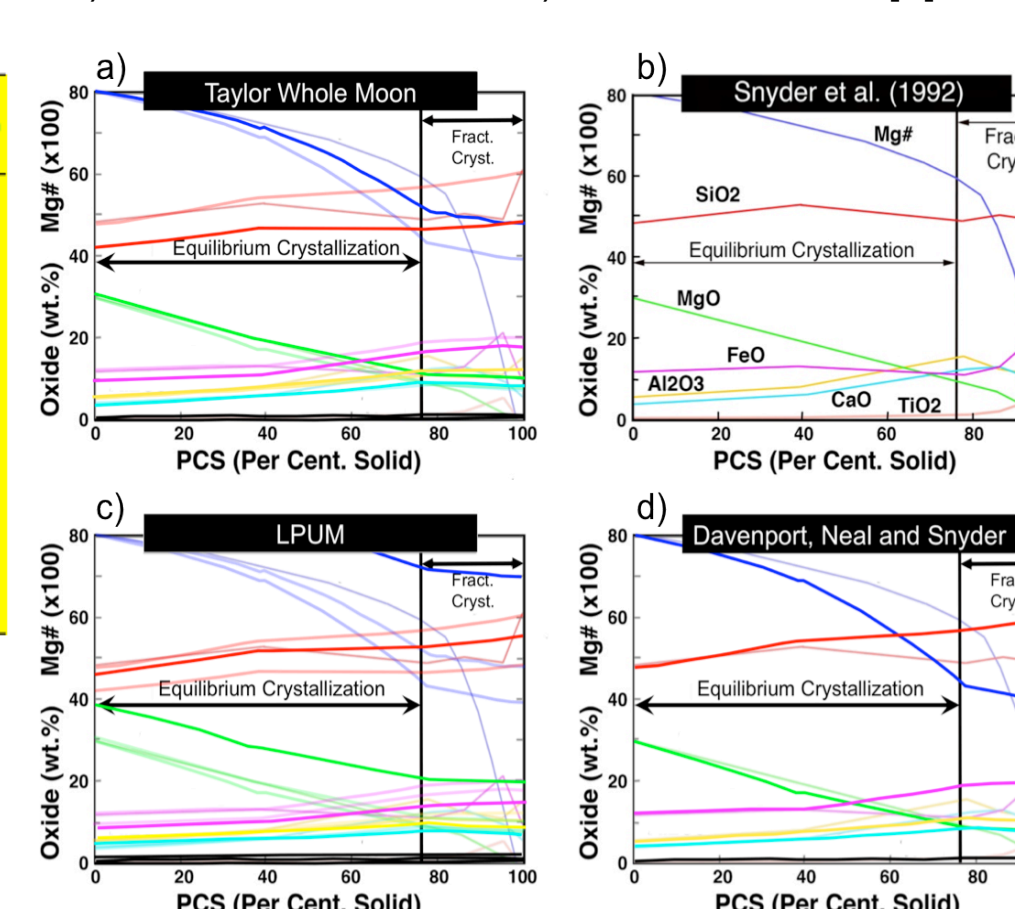


Figure 5 (left). Forward Monte Carlo modeling of the Lunar Magma Ocean. A range of compositions was generated from the literature, a normal distribution populated a set amount of numbers in that range and the program runs the predetermined amount of iterations resulting in a range of final LMO compositions (at 100 PCS).

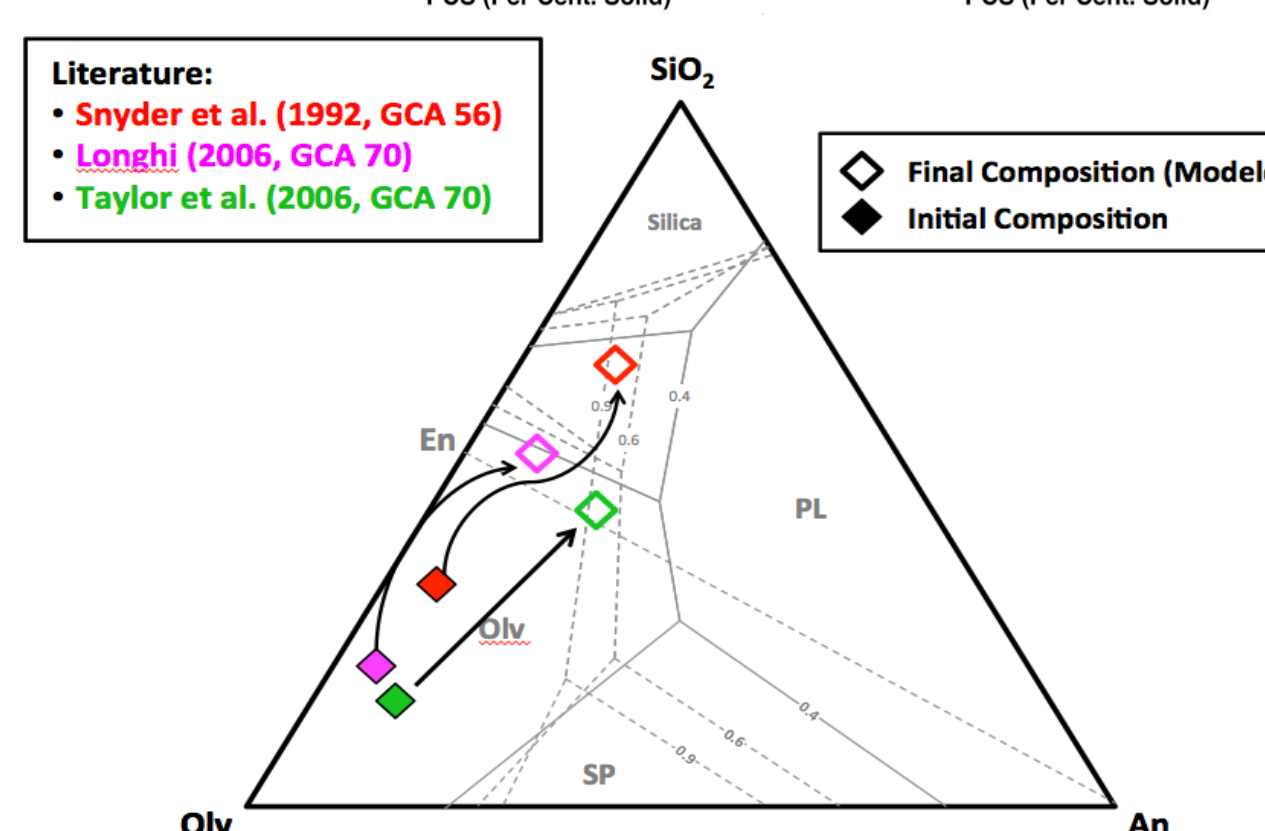


Figure 6 (right). A pseudo-ternary plot of Olivine, SiO₂ and anorthosite projected from Cpx plotting the Snyder [6], TWM and LPUM compositions in filled symbols and respective final compositions in open symbols.

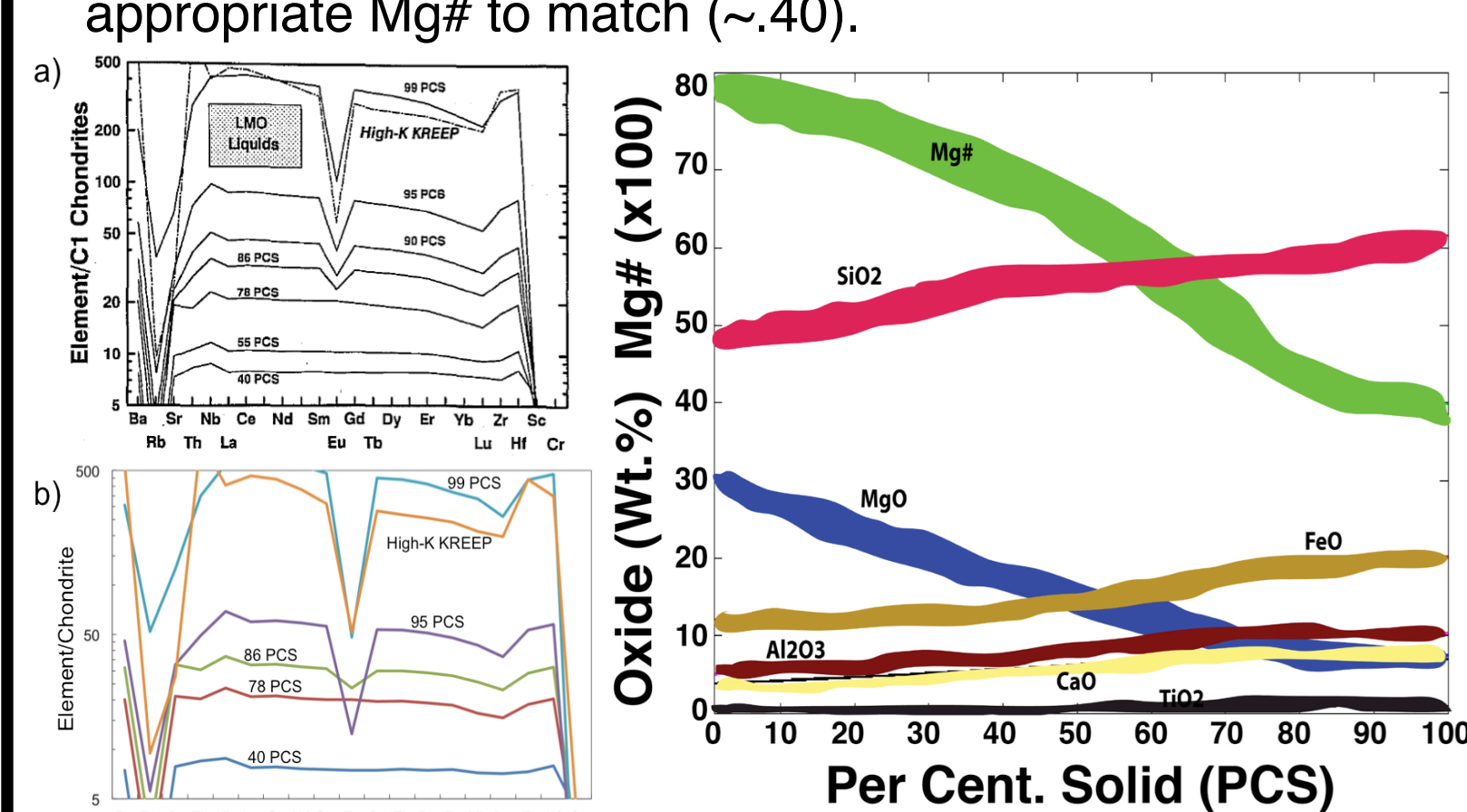


Figure 4 (above). Trace element evolution of the LMO. A) Original graph of [6] and B) this study's recreation of [6]'s trace element model.

Figure 9 (below). urKREEP compositions A) Warren & Wasson [10], B) Warren [21]; C) Warren [22]. Reversely modeled compositions give higher concentrations of Al₂O₃, TiO₂, & FeO.

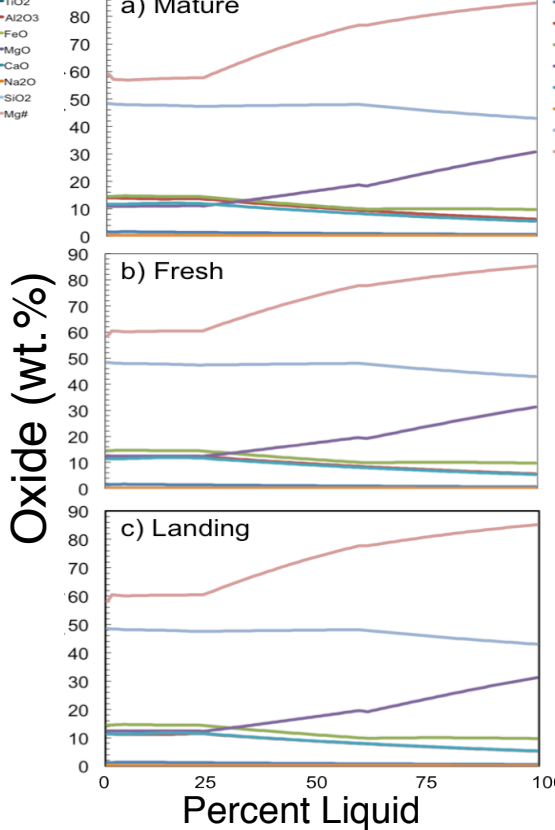
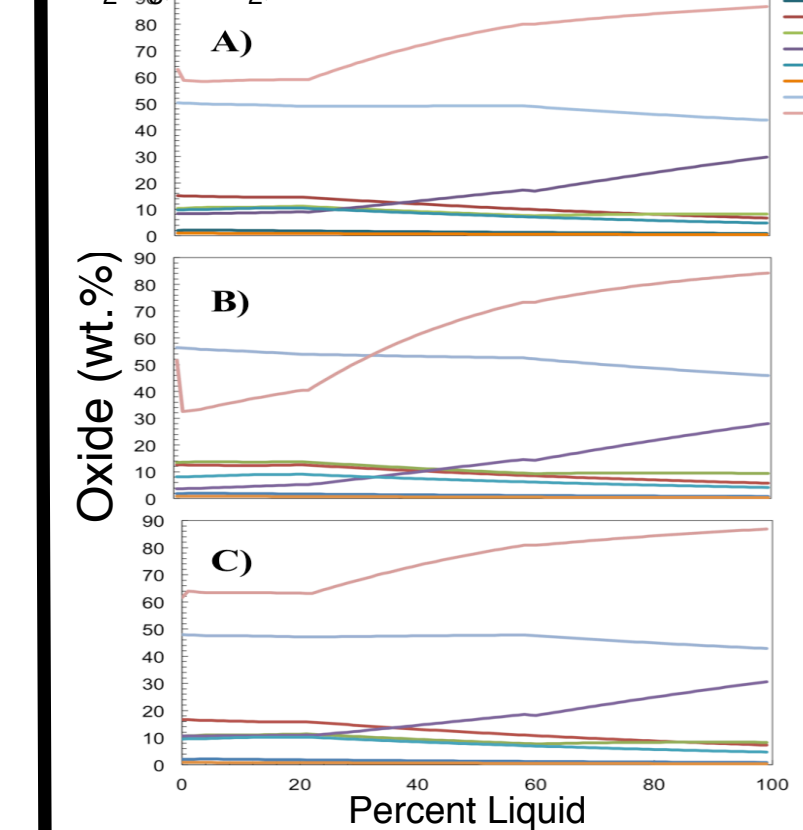
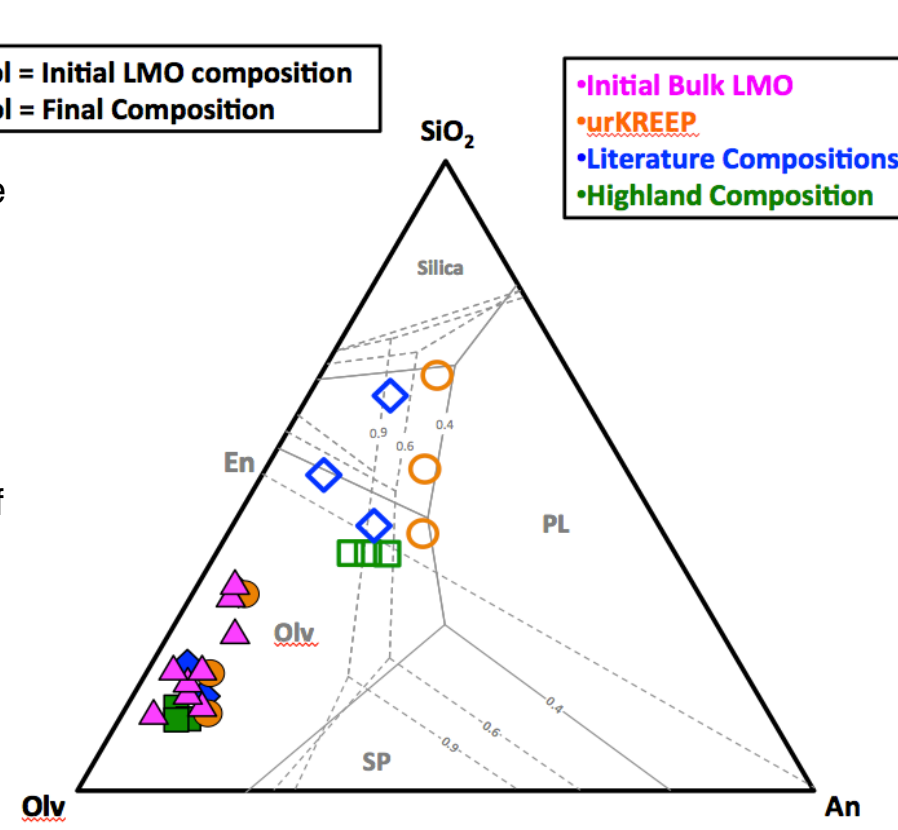


Figure 10 (left). A) Apollo 16 Mature site, B) Apollo 16 Fresh site and C) Apollo 16 Landing Site. Surface compositions provided by Shuai Li using the methods of [17] to calculate surface mineralogy.

Figure 12 (right). Pseudo-ternary of initial bulk LMO, urKREEP, literature and Highlands compositions. Open symbols represent final modeled compositions. Filled symbols represent bulk LMO and reversely modeled compositions.



Conclusions & Future Work

- Higher alumina content implies the following about the LMO and the Moon (needs to be reconciled with [14]):
 - Earlier crystallization of plagioclase
 - Hence, earlier formation of the crust, and insulating layer on surface
 - Longer-lived magma ocean because of the insulating lid
 - Earlier development of an europium anomaly, so is there a need for mantle overturn?
 - If the LMO ≥500 km garnet crystallizes in small quantities. Similar results were found by laboratory experiments in [20].
- Need updated partition coefficient databases.
- Need to incorporate other parameters such as any overturn event into model.
- Look at the global and local nature of the LMO through reverse modeling and procedures published in [17].

Acknowledgements

The authors would like to thank Brandon Schneider and Linda Elkins-Tanton for their help with MATLAB code and implementation. This work is supported by NASA Cosmochemistry grant NNX09AB92G and NLSI subcontract via the LPI to Clive Neal.

References

[1] Wood et al. (1970) *Proc. Apollo 11 Lunar Sci. Conf.*, 965-988 [2] Smith et al. (1970) *Proc. Apollo 11 Lunar Sci. Conf.*, 897-925 [3] Elkins-Tanton L.T. et al. (2011) *EPSL* 304, 326-336 [4] Spera, F., (1992) *GCA* 56, 2253-2265 [5] Jolliff et al. (2000) *Eos. Trans. AGU*, 349-355 [6] Snyder G.A. et al. (1992) *GCA* 56, 3809-3823 [7] Davenport J. and C.R. Neal (2012) *43rd LPSC*, abstract #1546. [8] Davenport J. and C.R. Neal (2012) *Proc. NLSI LSF* [9] Davenport et al. (under review) *GCA* [10] Warren, P.H. and J.T. Wasson (1979) *Rev. Geophys. Space Phys.* 17, 73-88 [11] Davenport et al. (in prep.) *Comp. Geosci.* [12] Taylor et al. (2006) *GCA* 70, 5904-5918 [13] Longhi, J., (2006) *GCA* 70, 5919-5934 [14] Wiczorek et al., (2013) *Science* 339, 671-675 [15] Borg et al. (2011) *Nature* 477, 70-73 [16] Sakai et al. (2014) *Icarus* 229, 45-56. [17] Li, S. et al. (2012) *Icarus* 221, 208-225. [18] Neal C.R. and J.D. Davenport (2014, this conference) abstract #1181. [20] Elardo et al. (2011) *GCA* 75, 3024-3045. [21] Warren P. (1988) *PLPSC* 18, 233-241; [22] Warren P. (1989) *LPI Tech. Rpt.* 89-03, 149-153.